Phase-encoded computer-generated-hologram implemented with liquid crystal television

Ren-Chung Liu and Ken Y. Hsu

Institute of Electro-Optical Engineering, National Chiao Tung University, Taiwan, R.O.C.

ABSTRACT

The advantages of phase-encoded computer-generated-hologram (CGH) are high diffraction efficiency and the ability to reconstruct images on-axis. These advantages are very fundamental and important for many applications. The implementation of phase-encoded CGH by using electrical-addressable liquid crystal television (LCTV) with pure phase-modulation provides the ability for programmable optical interconnections, optical neural systems, optical switches etc. In this paper we adopt the iterative Fourier transform algorithm to design a pure phase CGH. We also report the modulation characteristics of LCTV and its application for displaying the phase-encoded CGH. Criterions for evaluating the quality of output images are proposed.

1. INTRODUCTION

Computer generated hologram (CGH) is a technique for fabricating holograms without optical interference process[1]. This technique consists of two steps: (1). Calculation of discrete Fourier transform of the desired image. (2). Encoding and fabrication of the calculated pattern on a suitable mask. The first step can be achieved efficiently by using fast Fourier transform (FFT) algorithm. The second step can be achieved by adopting certain encoding method and mask fabrication techniques. By use of modulation characteristics of spatial light modulators (SLM), the second step can be realized to become real-time programmable [2]. In the case, the complex pattern of CGH is displayed on a SLM and the reconstruction of CGH can be achieved by optical illumination of the SLM. Therefore, CGH can be real-time updated through the programmable control of the input pattern presented on the SLM. The modulation characteristics of a SLM can be divided into two types, the amplitude-modulation type and the phase-modulation type. The phase modulation type is preferable to the amplitude one because it provides higher diffraction efficiency and also with the ability to reconstruct the desired image on-axis. In this paper, we adopted the iterative Fourier transform algorithm (IFTA) to design CGH and use a liquid crystal television (LCTV) as the displaying device. We describe the modulation characteristics of LCTV and report computer simulations of phase-encoded CGH implemented with LCTV.

2. PRINCIPLES

CGH coefficients, generated by FFT of the desired image, are usually complex numbers. How to represent complex coefficients by a pure phase device is the main concern of phase encoding technique. Several methods have been proposed and demonstrated [3,4,5]. Basically, these methods require a technique to represent a distribution of phase information between 0 and 2π in analog mode, i.e., a continuous distribution of phase gray levels. This has brought in a practical difficulty for the implementation by using LCTV. Commercial LCTV has limited ranges of phase modulation, and it is difficult to have a precise modulation of gray levels between 0 and 2π. In order to alleviate this problem, we adopt the iterative Fourier transform algorithm (IFTA) [6,7,8] for designing the CGH. The advantage is that the solution of the phase encoded CGH is a distribution of discrete phase levels. The quantization of phase levels makes it more feasible to be implemented by using LCTV.

2.1 Designing phase-encoded CGH with IFTA

Fig.1 shows the schematic diagram of CGH and the reconstructed image. In the diagram, CGH is an optical mask to be designed so that the desired image can be reconstructed at the output plane. We call the CGH pattern in Fourier domain and the desired image to be reconstructed in space domain. The goal of the IFTA[8] is to generate a discrete phase pattern $\overline{W}(m,n)$ such that the desired image $I(m,n)$ can be retrieved by optical illumination of $\overline{W}(m,n)$.

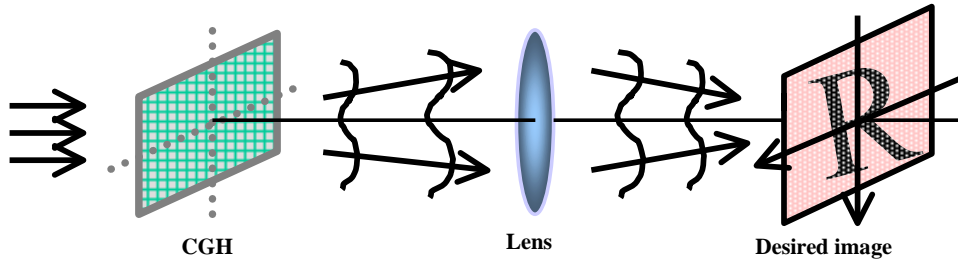**CGH**   **Lens**   **Desired image**

Fig. 1. Reconstruction of CGH

The block diagram of the IFTA iterations is shown in Fig.2. In the figure, $\overline{W}(m,n)$ represents the discrete phase pattern of CGH in Fourier domain, $w(m,n)$ is the reconstructed wave in space domain, and $A(m,n) = \sqrt{I(m,n)}$ is the desired image. During the iteration procedure, $\overline{W}(m,n)$ is continuously modified such that its Fourier transform $w(m,n)$ approaches the desired function $A(m,n)$. In order to achieve a pure phase-encoding result, there are specific constraints in the two domains. In the Fourier domain, the amplitude of all the $\overline{W}(m,n)$ elements are equalized to 1 and the phase terms of $\overline{W}(m,n)$ are quantized to become discrete phase-levels between 0 and 2π (for example, 8 or 16 levels). On the other hand, in the space domain, $w(m,n)$ is modified such that the error in amplitude between $w(m,n)$ and the desired function $A(m,n)$ is reduced. The up-date of the image function is described by the following equation

$$\overline{w}(m,n) = \left[|w(m,n)| + \alpha(m,n)\varepsilon(m,n) \right] \exp\left[j\phi(m,n) \right] \tag{1}$$

where

$$\varepsilon(m,n) = A(m,n) - |w(m,n)| \tag{2}$$

In the above equation, $\varepsilon(m,n)$ is the error between the reconstructed image and the desired image and $\alpha(m,n)$ is the error-correction factor, $0 < \alpha(m,n) \leqq 1$.

Now we describe the iterative procedure. In the beginning, an arbitrary phase pattern $\overline{W}(m,n)$ is given in the CGH plane. By taking the Fourier transform of the initial random phase pattern, we obtain the reconstructed image in the image plane. Then, the amplitude of the reconstructed function is modified according to Eq.(1). The phase of the reconstructed function is retained unchanged. The combination of the modified amplitude and phase forms the modified image function $\overline{w}(m,n)$. By taking the inverse Fourier transform of $\overline{w}(m,n)$, we obtain a new pattern $W(m,n)$. In order to be a pure phase pattern, the amplitude of all elements of $W(m,n)$ are set to be unity, and the phase is discretized. Combination of the unitary amplitude and the discretized phase forms a new pattern $\overline{W}(m,n)$. Then, this pattern is compared with the input pattern for previous iteration. If they are identical then this means that a stable state has been reached and it is the solution for our CGH. Otherwise, the new $\overline{W}(m,n)$ is the input for next iteration. The iteration procedure continues until it converges, and the final pattern is the solution of our CGH.
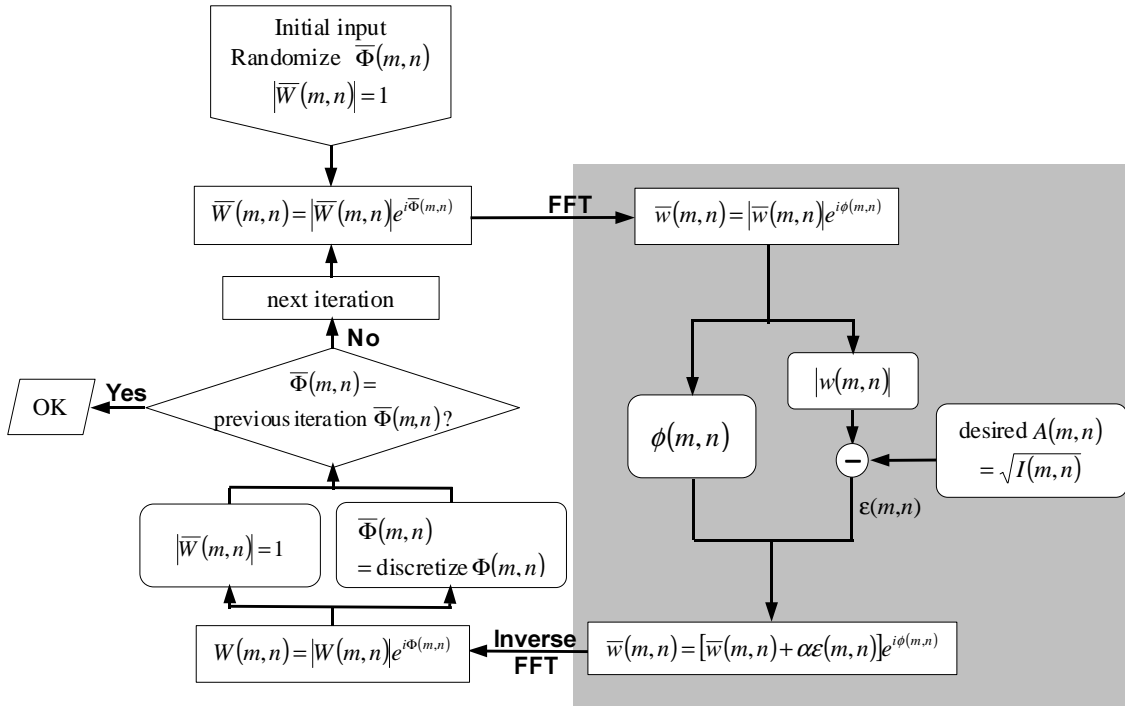
Fig. 2. Block diagram of IFTA

3. COMPUTER SIMULATIONS

We use a character "R", a binary pattern with 50x50 pixels, as the desired image, as shown in Fig.3. We assume the light transmission of the pixels of the character "R" to be 1, and it is 0 for all other pixels.

Fig. 3. Character " **R** ", the desired image.

In order to evaluate the image quality produced by CGH, we define three parameters. First, we define the diffraction efficiency η % as the ratio of the total energy inside the character "R" to the total energy in the output plane, It is described by

$$\eta \% = \frac{\sum\limits_{(m,n)\in R} |w(m,n)|^2}{\sum\limits_{all\,(m,n)} |w(m,n)|^2} \times 100\,\%$$
(3)

Second, we define the signal to noise ratio as the ratio of the average light energy inside the character "R" to the average energy outside the character. The SNR is described by

$$SNR = \frac{\sum_{(m,n)\in R}|w(m,n)|^2 \Big/ (\text{pixel number inside R})}{\sum_{(m,n)\notin R}|w(m,n)|^2 \Big/ (\text{pixel number outside R})} \qquad (4)$$

Finally, the error rate is defined as the average value of the energy error of the reconstructed image, averaged over all pixels. It is written by

$$ER\% = \frac{\sum_{all(m,n)}\left||A(m,n)|^2 - |w(m,n)|^2\right|}{\text{total pixel number}} \cdot 100\% \qquad (5)$$

3.1 Simulation results

In our simulations, we consider three cases of the phase quantization: 8, 16, and 256 discrete levels for 2π. Finer phase levels may produce a better image but it will result in either more iterations for designing CGH or more complexity in manipulating SLMs. Fig.4 shows convergence of the error rate versus iteration loop numbers. It is seen that for all three cases the solution converges very quickly.
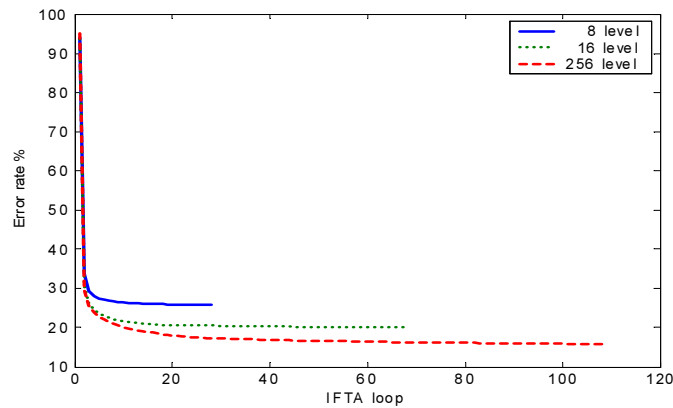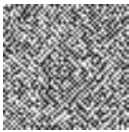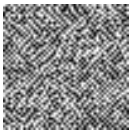

Fig. 4. The error rate versus IFTA loop number.

For the case with 8 phase levels, the solution converges in about 28 loops, and it converges to a state at an error rate of 25.7%. For the solution with 16, and 256 phase levels, the iteration converged at 68 and 109 loops, with the error rates of 20.1% and 15.8%, respectively. The phase patterns, the reconstructed images, the diffraction efficiencies, SNR, and the ER for the three cases are shown in Table.1. In the second column of this table, the phase levels of the CGH are represented by the gray scale of the color. It is seen that as the number of phase levels is increased, the image quality, the diffraction efficiency, SNR, as well as ER are improved.

Levels of Discretization	CGH	Reconstructed Image	η%	SNR	ER%
8			83.23	31.01	25.7
16			87.93	45.52	20.1

256		R	92.26	74.45	15.8

Table 1. CGH patterns, reconstructed images, diffraction efficiencies, SNR, and ER for the three cases.

4. IMPLEMENTATION BY LCTV DISPLAY

4.1   Phase modulation characteristics of LCTV

The main component of a LCTV is a liquid crystal panel, which is sandwiched between a polarizer and an analyzer, as shown in Fig.5. Let the polarization angle of the polarizer be Ψ_P, the polarization angle of the analyzer be Ψ_A, with respect to the x-axis. By applying the Jones calculus, the transmitted light can be found as

$$M_A \cdot M_L \cdot \begin{bmatrix} \cos \Psi_P \\ \sin \Psi_P \end{bmatrix} = A \cdot e^{j\psi} \cdot \begin{bmatrix} \cos \Psi_A \\ \sin \Psi_A \end{bmatrix} \tag{6}$$

In the above expression, M_A and M_L and are the Jones matrix of the analyzer and LC panel, respectively. The intensity and phase of the transmitted light can be written as

$$|A|^2 = [\phi \frac{\sin X}{X} \cos(\Psi_P - \Psi_A) - \cos X \sin(\Psi_P - \Psi_A)]^2 + [\frac{\Gamma}{2} \frac{\sin X}{X} \sin(\Psi_P + \Psi_A)]^2 \tag{7}$$

$$\psi = \beta - \tan^{-1} \frac{-\frac{\Gamma}{2} \frac{\sin X}{X} \sin(\Psi_P + \Psi_A)}{\varphi \frac{\sin X}{X} \cos(\Psi_P - \Psi_A) - \cos X \sin(\Psi_P - \Psi_A)} \tag{8}$$

where
$$X = \sqrt{\varphi^2 + \left(\frac{\Gamma}{2}\right)^2} \tag{9}$$

$$\Gamma = \frac{2\pi}{\lambda}(n_e(\theta) - n_o)d = \frac{2\pi}{\lambda}\Delta n(\theta)d \tag{10}$$

$$\beta = \frac{2\pi}{\lambda}(n_e(\theta) + n_o)d \tag{11}$$

λ is the light wavelength, n_e is refractive index for extraordinary ray, n_o is refractive index for ordinary ray, φ is the twisted angle of the twisted nematic LC cell, and d is the LC film thickness. For a specific LCTV with the oriented polarizer and analyzer, the device parameters are all fixed. The only parameter that is real-time adjustable is the extra-ordinary refractive index $n_e(\theta)$, which is a function of the tilt angle θ of LC molecules and it in turn can be controlled by the external voltage applied to LCTV. Thus, by applying different voltages to LCTV the modulation characteristics is real-time programmable. In our simulation, we set Ψ_P to be 0^0, Ψ_A to be 90^0, the twisted angle φ to be 90^0, $n_e = 1.856$, $n_o = 1.561$, and film thickness to be 6μm. The modulation characteristics of the LCTV are shown in Fig.6. Note that, in this figure, the modulation characteristics are shown as a function of the phase retardation Γ, which can be adjusted by applying voltages on the LC panel.
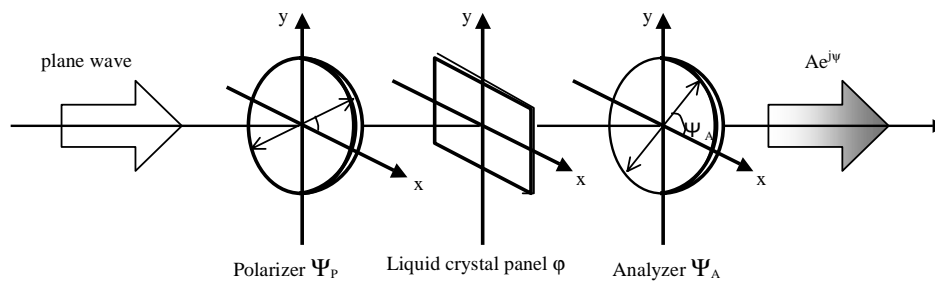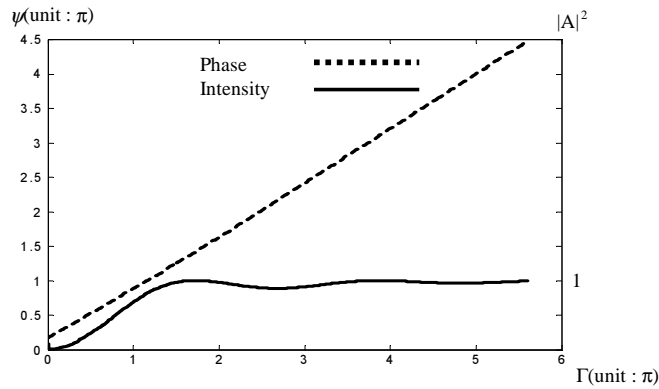

Fig. 5. LCTV as a SLM

Fig.6. Modulation characteristics of LCTV

It can seen in Fig.6 that when Γ is tuned between 1.5π to 4.5π, the phase is modulated from about π to 3π, and the output intensity is almost a constant. In this region, LCTV can operate as a phase modulation device.

4.2 Phase-encoded CGH implemented with LCTV

The liquid crystal panel is not uniformly transparent within the whole device area because part of its area is covered with electrical circuits. The schematic diagram of pixel structure is shown in Fig.7, in which the gray area represents the electrical circuits and is opaque. Let the pixel pitch be represented by Δ and the width of the transparent window be δ, then a mathematical representation of phase-encoding CGH displayed on LCTV can be written as
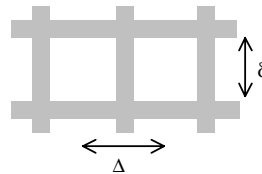

Fig. 7. Light transmission structure of LC pixels.

$$H(u,v) = \sum_{m=0}^{M-1}\sum_{n=0}^{N-1}\overline{W}(m,n)rect(\frac{u}{\delta})rect(\frac{v}{\delta}) \otimes \delta(u - m\Delta, v - n\Delta) \qquad (12)$$

where $\overline{W}(m,n)$ is the matrix element of the CGH pattern obtained by the IFTA algorithm. Let the LCTV be placed in the (u, v) plane, being illuminated by a plane wave, and the reconstructed image be formed at the (x, y) plane, as shown in Fig.8. The reconstructed image can be written as
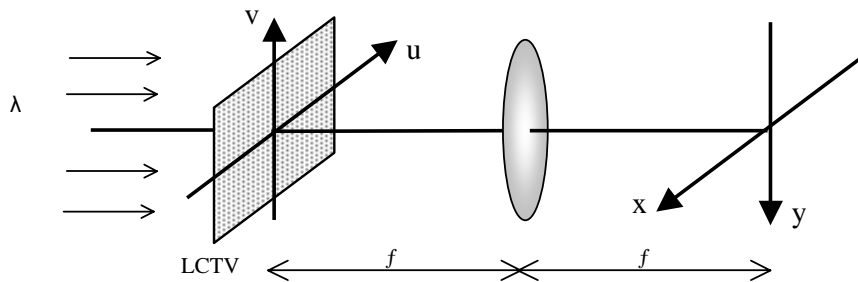

Fig.8.   Optical reconstruction of the CGH.

$$h(x, y) = \frac{1}{\lambda f} \iint H(u,v) rect(\frac{u}{M\Delta}) rect(\frac{v}{N\Delta}) \exp[-j\frac{2\pi}{\lambda f}(ux + vy)]dudv$$

$$\propto \left(\sin c(\frac{\delta x}{\lambda f}) \sin c(\frac{\delta y}{\lambda f}) \sum_{m=0}^{M-1}\sum_{n=0}^{N-1} \overline{W}(m,n) \exp\left[j\frac{2\pi\Delta}{\lambda f}(mx+ny) \right] \right) \otimes \sin c(M\frac{\Delta x}{\lambda f}) \sin c(N\frac{\Delta y}{\lambda f}) \tag{13}$$

The above equation shows that the amplitude of the reconstructed image is enveloped by sinc functions, $\sin c(\delta x/\lambda f)$ and $\sin c(\delta y/\lambda f)$. It also shows that the spot size of the reconstructed image is about $\lambda f/M\Delta$. In our calculation, we choose wavelength λ to be 633 nm, the LCTV pitch 33 μm, the width of transparent window 24 μm, and lens focus length 15 cm. The reconstructed image is shown in Fig.9.

Fig. 9 Reconstructed image.

5. CONCLUSIONS

We have investigated the designing principle of phase CGH and the modulation characteristics of LCTV. We have described an iterative Fourier transform algorithm for the design of phase-encoded CGH with discrete phase levels. We have performed three cases of phase quantizations with 8, 16, and 256 phase levels, respectively. The results show that as the quantization level is increased, the image quality is improved, with an increasing complexity of calculation. We have described the modulation characteristics of LCTV. It is shown that under certain conditions a real-time pure-phase modulation of LCTV can be achieved. A computer simulation of the phase-encoded CGH implemented with LCTV has been demonstrated.

6. ACKNOWLEDGEMENT

REFERENCES

1. B. R. Brown and A. W. Lohmann, " Complex Spatial Filter, " *Appl. Opt.* **5**, p. 967, 1966.
2. Francis T. S. Yu, Suganda Jutamulia, Tsongneng W. Lin, Don A. Gregory, "Adaptive real-time pattern recognition using a liquid crystal TV based joint transform correlator," *Appl. Opt.*, **26**, p. 1370, 1987.
3. L. B. Lesem, P. M. Hirsch, and J. A. Jordan, Jr., "The kinoform:a new wavefront reconstruction device," *IBM J. Res. And Dev.*, **13**, p. 150, 1969.
4. J. M. Florence and R. D. Juday, "Full-complex spatial filtering with a phase mostly DMD," *Proc. SPIE*, 1558, p. 487, 1991.
5. D. Mendlovic, G. Shabtay, U. Levi, Z. Zalersky, and E. Marom, "Encoding technique for design of zero-order (on-axis) Fraunhofer computer-generated-holograms," *Appl. Opt.*, **36**, p.8427, 1997
6. J. R. Fienup, "Phase retrieval algorithm: a comparison, " *Appl. Opt.*, **21**, p. 2758, 1982
7. F. Wyrowski and O. Bryngdahl, "Iterative Fourier transform algorithm applied to computer holography," *JOSA. A*, **5**, p. 1058, 1988.
8. Matthias Gruber, " Diffractive optical elements as raster-image generator, " *Appl. Opt.*, **40**, p. 5830, 2001.